Applied Catalysis B: Environmental 99 (2010) 353–363

Contents lists available at ScienceDirect

Applied Catalysis B: Environmental

journal homepage: www.elsevier.com/locate/apcatb

The role of lattice oxygen on the activity of manganese oxides towards the oxidation of volatile organic compounds

V.P. Santos, M.F.R. Pereira, J.J.M. Órfão, J.L. Figueiredo *

Laboratório de Catálise e Materiais (LCM), Laboratório Associado LSRE/LCM, Departamento de Engenharia Química, Faculdade de Engenharia, Universidade do Porto, Rua Dr. Roberto Frias, 4200-465 Porto, Portugal

ARTICLE INFO

Article history:
Received 17 May 2010
Received in revised form 28 June 2010
Accepted 6 July 2010
Available online 15 July 2010

Keywords:
Manganese oxides
Cryptomelane
Oxidation
Volatile organic compound
Ethanol
Toluene
Ethyl acetate

ABSTRACT

A series of manganese oxides differing in the structure, composition, average manganese oxidation state and specific surface area have been used in the total oxidation of volatile organic compounds (VOC). Ethanol, ethyl acetate and toluene were chosen as models of VOC.

Among the manganese oxides tested, cryptomelane (KMn_8O_{16}) was found to be very active in the oxidation of VOC. The performance of cryptomelane was significantly affected by the presence of other phases, namely, Mn_2O_3 and Mn_3O_4. Temperature-programmed experiments combined with X-ray photoelectron spectroscopy (XPS) show that the mobility and reactivity of the oxygen species were significantly affected, explaining the catalytic performances of those samples. Mn_3O_4 improves the catalytic performance due to the increase of the reactivity and mobility of lattice oxygen, while Mn_2O_3 has the opposite effect. These results show that there is a correlation between the redox properties and the catalytic performance of the manganese oxides.

Temperature-programmed surface reactions (TPSR) after adsorption of toluene or ethanol, in addition to reactions performed without oxygen in the feed, show that lattice oxygen is involved in the VOC oxidation mechanism. The conversion level was found to be influenced by the type of VOC, the reactivity into CO_2 increasing in the following order: Toluene < Ethanol < Ethyl Acetate. The type of VOC is particularly important, as each VOC affects the reduction of the catalyst and, consequently, the incorporation rate of oxygen from the gas phase. Toluene decreases the oxygen mobility, so there is a slower incorporation rate of oxygen in the lattice, which explains the lower conversions observed.

1. Introduction

Tunnel structured manganese oxides are promising catalysts for the total oxidation of volatile organic compounds (VOC) [1–6]. Their high activity is ascribed to the open tunnel structure, the mixed valence character of manganese, and the high mobility of lattice oxygen [7–11].

The synthesis and properties of bulk cryptomelane (KMn_8O_{16}) materials have been intensively studied in the past [12–14]. Synthesis methods include thermal and hydrothermal treatment of layered birnessite [15], redox precipitation under reflux [1,16], microwave heating [17], sol–gel methods [18] and a solvent-free procedure [19]. Among them, the reflux method, involving the oxidation of Mn^{2+} by MnO_4^-, is the most common route.

In a previous report [4], our group studied the influence of pH and the template cation on the formation of this kind of structure. The reflux method was the procedure adopted. The crystallinity and microstructure of cryptomelane largely depended on the nature of the template, while the template concentration was found to be an important parameter to prevent the formation of Mn_3O_4, Mn_5O_8 and Mn_2O_3 as by-products. Several manganese oxides, differing in their crystallinity, structure, average oxidation state and surface area were obtained. The activity of these materials was tested in the total oxidation of ethyl acetate, all samples being able to oxidise this VOC into CO_2 at low temperatures. Cryptomelane doped with small amounts of Mn_3O_4 showed the best performance.

The aim of the present paper is to study the oxidation of ethanol and toluene over the same catalysts, and to provide a better understanding of the VOC oxidation mechanism over manganese oxides. The oxidation of organic molecules over this type of catalyst usually proceeds according to the Mars and van Krevelen (MVK) mechanism, where the organic molecule is oxidised by the lattice oxygen of the oxide, the latter being re-oxidised by gas phase oxygen. Therefore, the availability and reactivity of surface oxygen species provide a method for the identification of the most active catalyst. The oxygen species in manganese oxides were studied in detail by temperature-programmed experiments in combination

* Corresponding author. Tel.: +351 22 508 1663; fax: +351 22 508 1449.
E-mail addresses: santos.vera@fe.up.pt (V.P. Santos), fpereira@fe.up.pt (M.F.R. Pereira), jjmo@fe.up.pt (J.J.M. Órfão), jlfig@fe.up.pt (J.L. Figueiredo).

0926-3373/$ – see front matter © 2010 Elsevier B.V. All rights reserved.
doi:10.1016/j.apcatb.2010.07.007

Table 1
Properties of the catalysts: average oxidation states (obtained by XPS), surface areas (obtained by nitrogen adsorption) and crystalline phases (obtained by XRD).

Sample	AOS	S_{BET} (m^2/g)	Phases
Mn2	3.89	71	KMn_8O_{16}
Mn4	3.74	45	KMn_8O_{16}; α-Mn_2O_3
Mn5	3.72	84	KMn_8O_{16}; Mn_3O_4
Mn6	3.74	59	KMn_8O_{16}; α-Mn_2O_3; Mn_5O_8
Mn7	3.78	46	α-Mn_2O_3; β-MnO_2

with X-ray photoelectron spectroscopy (XPS), in order to correlate catalyst activities with their properties.

2. Experimental

2.1. Catalysts synthesis and characterization

Five manganese oxides with different structures, surface areas and manganese average oxidation states were prepared as described in a previous work [4]. All samples were prepared by the reflux method, according to Ref. [1]. Samples Mn2 and Mn4 were prepared with $KMnO_4$, the initial pH being 3.5 for Mn2 and 2.0 for Mn4. Samples Mn5 and Mn6 were prepared with a buffer solution (KCH_3COO/CH_3COOH) at pH 4.5. $NaMnO_4$ was the oxidant in Mn5, while $CsMnO_4$ was used in Mn6. Sample Mn7 was prepared with $NaMnO_4$ at initial pH 4.5. HNO_3 was used to adjust the initial pH in samples Mn2, Mn4 and Mn7.

The structure, morphology, composition, manganese average oxidation state (AOS), texture and stability of the prepared samples were fully characterized by X-ray diffraction (XRD), scanning electron microscopy/energy dispersive X-ray spectroscopy (SEM/EDS), XPS, N_2 adsorption at −196 °C, thermogravimetric analysis (TGA) and temperature-programmed desorption (TPD). A summary of the catalysts properties is presented in Table 1.

This paper is focused on the study of the oxygen species in the tunnel structured manganese oxides by TPD and temperature-programmed reduction (TPR), combined with XPS. The fractions of Mn(II), Mn(III) and Mn(IV) species, for each sample, were obtained by XPS.

2.1.1. Temperature-programmed experiments (TPD and TPR)

These experiments were carried out in an Altamira Instruments (AMI 200) apparatus.

For TPD, 100 mg of each sample were loaded into the sample holder and placed inside the furnace. The sample was purged with helium for 1 h at room temperature followed by heating to 900 °C at 5 °C/min in the same atmosphere. Evolution of oxygen from the sample was monitored with a mass spectrometer (MS).

A mixture of 10 vol.% H_2/He was used for TPR experiments, at a total flow rate of 30 cm^3/min, with 50 mg of catalyst. The temperature was increased at a rate of 10 °C/min from room temperature to 600 °C, while the hydrogen consumption was monitored.

2.1.2. X-ray photoelectron spectroscopy

XPS analysis was performed with a VG Scientific ESCALAB 200A spectrometer using Al Kα radiation (1486.6 eV). Charge effects were corrected by adjusting the binding energy of C 1s to 284.6 eV.

2.2. Catalytic activity measurements

The catalytic oxidation of VOC was performed under atmospheric pressure in a fixed-bed reactor from Autoclave Engineers (BTRS Jr), which consists of a stainless steel tube of 6 mm internal diameter, placed inside a temperature-controlled electric furnace. A feed gas with a VOC concentration of 4000 mg C/m^3 and a space velocity of 16,000 h^{-1} was used in standard tests. The catalyst sample (50 mg) was diluted with glass spheres of the same size as the catalyst particles (0.2–0.5 mm), in order to minimize temperature gradients.

Conversions were measured over the range 100–350 °C by incremental steps (10–20 °C), the temperature being measured by a thermocouple placed in the middle of the catalyst bed. To ensure that steady state data were measured, the reactor was maintained at each temperature for 30 min. The conversion of VOC (X) and the conversion into CO_2 (X_{CO_2}) were respectively calculated as $X = 1 - F_{VOC}/F_{VOC,in}$ and $X_{CO_2} = F_{CO_2}/\nu F_{VOC,in}$, where F_{VOC} is the outlet molar flow rate of VOC at steady state, $F_{VOC,in}$ is the inlet molar flow rate of VOC, F_{CO_2} is the outlet molar flow rate of CO_2 at steady state and ν is the number of carbon atoms in the VOC molecule (for ethanol, ethyl acetate and toluene, $\nu = 2$, 4 and 7, respectively).

Duplicate experiments with selected samples showed that the maximum deviation was ± 4 °C.

2.3. Temperature-programmed surface reactions (TPSR) and reactions without oxygen in the feed

TPSR experiments were conducted in an Altamira Instruments (AMI 200) apparatus. 100 mg of each sample were loaded into the sample holder and placed inside the furnace. The adsorption of VOC (ethanol or toluene) was carried out at room temperature, using a concentration of 4000 mg C/m^3. After saturation, the system was purged with helium and the experiment started. The temperature was increased at 10 °C/min to 600 °C. The products were analysed by MS.

Reactions without oxygen in the feed were carried out in a fixed-bed reactor from Autoclave Engineers (BTRS Jr). The experimental conditions used here were the same as described in Section 2.2 (4000 mg C/m^3 and 16,000 h^{-1}). Prior to the reaction the catalyst was activated in air at selected reaction temperatures (210 or 270 °C, for ethanol or toluene, respectively). The reactor was then purged with nitrogen in order to remove physisorbed oxygen, and the experiment started. Additional experiments were carried out with a selected sample (Mn5) varying the activation time, which was 10 min in the first cycle, and 5, 2 and 1 min in the following cycles.

3. Results and discussion

3.1. Characterization

The oxygen species present in the MnO_x materials were completely characterized by temperature-programmed studies (TPD and TPR) and XPS.

3.1.1. Temperature-programmed studies

TPD and TPR techniques have proved to be very useful to investigate oxygen species of single and mixed oxides, throwing light on the type of oxygen species and their properties, such as reactivities [20–23]. According to Yin et al. [20], three types of oxygen species can be identified in the tunnel structured manganese oxides, according to their peak positions in TPD/TPR spectra: the α-species, which are weakly bound to the surface (usually O_2^- and O^- surface oxygen species), and the β and γ species, assigned to lattice oxygen. The β and γ species are differentiated by the binding strengths between manganese and oxygen. Oxygen atoms in the framework bound to Mn(III) have a weaker interaction, and are released in the middle temperature range during TPD, while the oxygen atoms bound to Mn(IV) are released at higher temperatures, and are assigned as γ species.

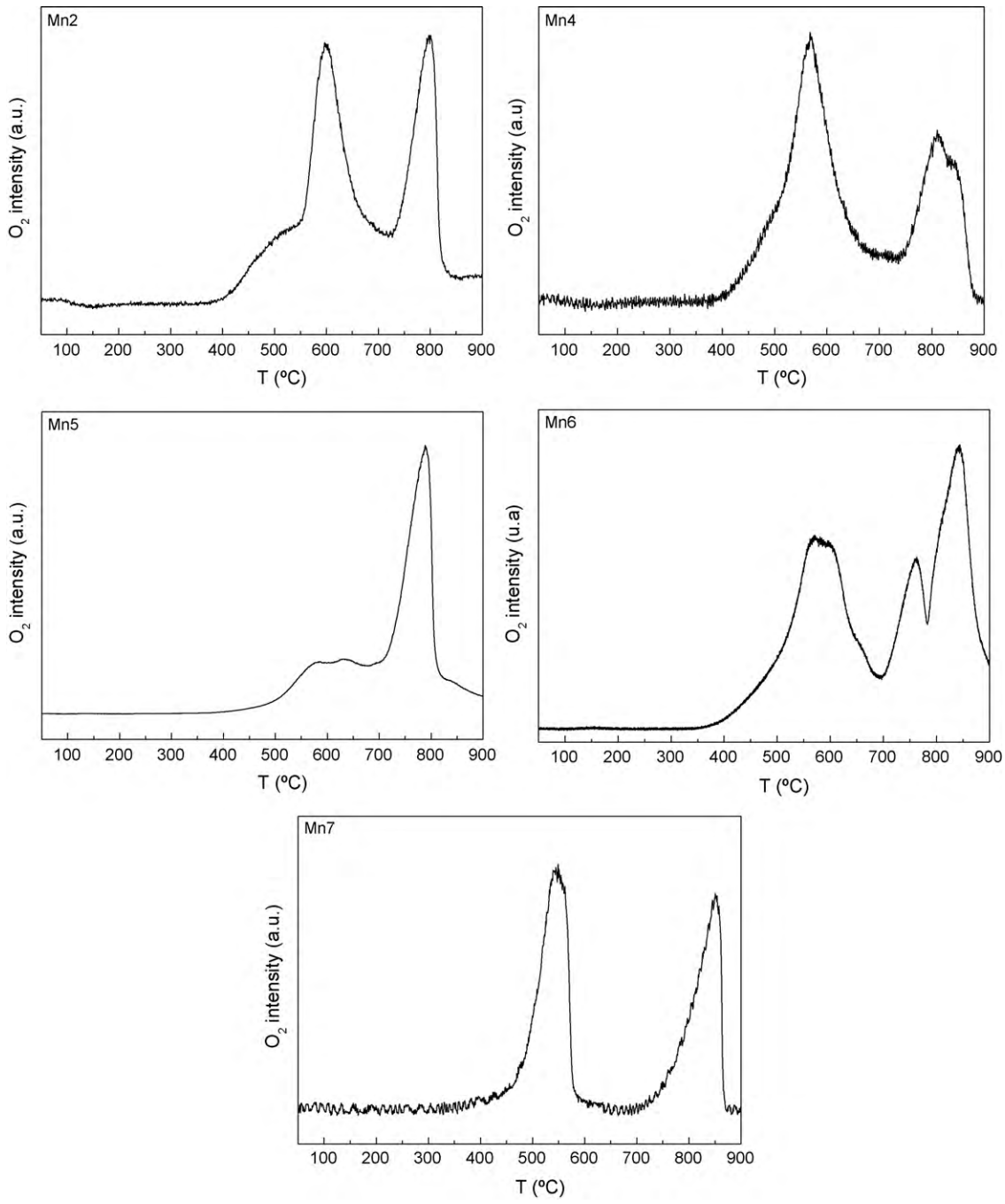

Fig. 1. Oxygen TPD spectra of the MnO_x catalysts. Heating rate: 5 °C/min.

3.1.1.1. Temperature-programmed desorption. The TPD-O_2 profiles of the MnO_x materials are presented in Fig. 1. The majority of the oxygen species in all samples can be ascribed to lattice oxygen, in agreement with other authors [20,22].

The O_2 pattern of Mn2 is characterized by two peaks at about 600 and 800 °C. The first peak exhibits a clear shoulder that can result from desorption of surface oxygen species (O^- and O_2^-) and/or the presence of labile oxygen species (β species), with different Mn–O bond strengths. According to the literature [3,24] and confirmed by TGA [4], the first peak is assigned to the transformation of cryptomelane to Mn_2O_3 (responsible for a weight loss of 7%), while the second peak corresponds to the subsequent reduction to Mn_3O_4 (2.6% weight loss):

$$KMn_8O_{16} \rightarrow Mn_2O_3 \rightarrow Mn_3O_4$$

A similar pattern was obtained for the Mn4 sample, but the temperature of the first peak is shifted to lower temperatures (≈550 °C), showing lower stability. The differences in the stability between Mn2 and Mn4 samples can be explained by the structural changes caused by the presence of the Mn_2O_3 phase. Moreover, an additional peak at higher temperatures (840 °C) suggests an intermediate transformation. A shoulder is also present in the lower temperature peak, although not so evident as in the case of the Mn2 sample.

The O_2 profile of the Mn5 sample is quite different from the Mn2 and Mn4 samples. The lower temperature peak (maximum near 600 °C) is less intense, and is also ascribed to desorption of α and β species. In this case, the transformation of cryptomelane to Mn_2O_3 does not occur. The higher temperature peak is also ascribed to the transformation of cryptomelane to Mn_3O_4. Compared to the pure cryptomelane sample (Mn2), Mn5 has a higher stability (the

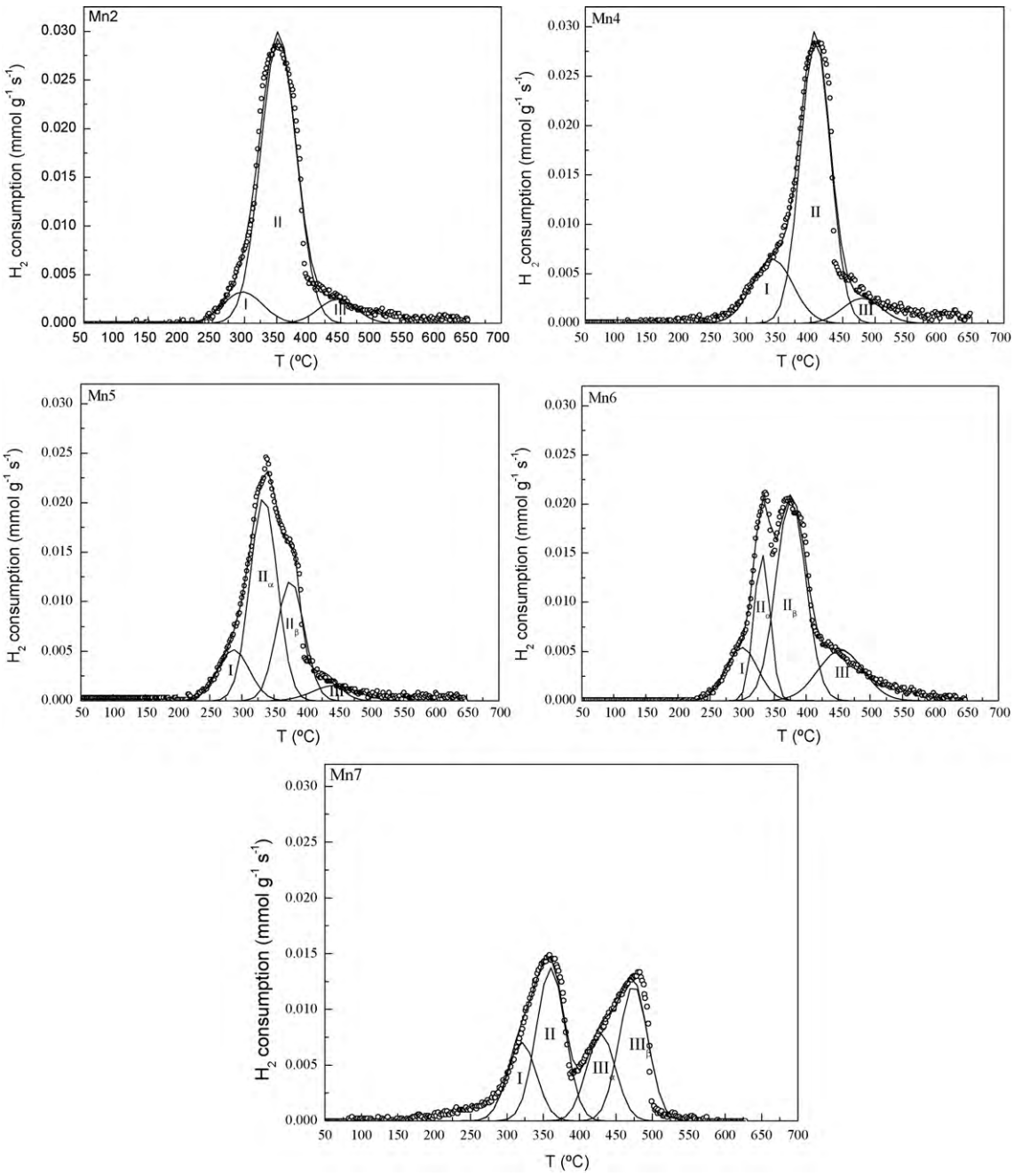

Fig. 2. TPR profiles of the MnO_x catalysts. Heating rate: 10 °C/min.

first peak is shifted to higher temperatures), which means that the presence of Mn_3O_4 has a pronounced effect on the stability of the oxygen species.

The oxygen spectrum of Mn6 is more complex, showing three peaks between 400 and 900 °C, assigned to three intermediate transformations.

The last sample shows a different behaviour as a result of its different structure and composition. Two major peaks at 550 and 850 °C are observed, as a result of the successive transformations to Mn_2O_3 and Mn_3O_4.

In summary, the structural changes caused by the presence of the phases Mn_2O_3, Mn_3O_4 and Mn_5O_8 in cryptomelane play a decisive role on the stability of the materials, affecting the mobility of lattice oxygen. The different shapes of the oxygen TPD profiles resulted also from the presence of different manganese species (Mn(II), Mn(III), Mn(IV)).

3.1.1.2. Temperature-programmed reduction. The reactivity of the oxygen species was studied by TPR. According to Kapteijn et al. [25], the reduction of manganese oxides can be described by the successive processes:

$$MnO_2 \rightarrow Mn_2O_3 \rightarrow Mn_3O_4 \rightarrow MnO$$

However, the peaks on the TPR curves may also result from reduction of species in different local environments [26]. Fig. 2 shows the reduction profiles of the MnO_x samples. Each profile was decomposed into three or four components, depending on the sample, and the corresponding positions are summarized in Table 2. The deconvolution procedure included the following steps: (i) selecting the minimum number of peaks which could describe each profile; (ii) fitting the profiles by imposing the same full width at half maximum (FWHM) for all component peaks; (iii) optimising the deconvolution by allowing small deviations in the FWHM.

Table 2
Position of the TPR components (°C) for the MnO_x catalysts.

Sample	Peak I	Peak II		Peak III	
		Peak II_α	Peak II_β	Peak III_α	Peak III_β
Mn2	296	352		445	
Mn4	340	407		488	
Mn5	284	339	383	425	
Mn6	300	333	374	456	
Mn7	320	360		430	480

The TPR spectrum of the Mn2 sample is characterized by a large peak with a maximum at about 350 °C. A shoulder clearly appears at the end of the peak, which may indicate that the reduction proceeds in two steps:

$$KMn_8O_{16} \rightarrow Mn_3O_4 \rightarrow MnO$$

This result is in agreement with other authors [27]. Moreover, the shoulder at low temperatures reveals the presence of labile species with different Mn–O strengths, in agreement with the TPD results. Those species are not strongly stabilized within the oxide lattice, and can be regarded as the surface reactive species.

A similar reduction pattern is obtained for the Mn4 sample, but the temperature of the main peak is shifted to higher temperatures (see Table 2), showing lower reducibility (thus, lower reactivity). Moreover, the low temperature shoulder is larger in comparison to the Mn2 sample, due to the lower AOS (and consequently higher relative amounts of Mn(III) species).

The reduction profiles of Mn5 and Mn6 are different from those observed on the two previous samples. The spectra are characterized by the presence of two overlapping components with maxima around 335 and 380 °C, suggesting that an intermediate reduction into Mn_2O_3 takes place. Shoulders also appear at the beginning and at the end of the mentioned peaks. The main difference between the Mn5 and Mn6 samples is the intensity of the component peaks II_β and III (which are much larger in the Mn6 sample) and the position of component I. In fact, the reduction of Mn5 starts at lower temperatures, having higher reducibility.

The TPR spectrum of the Mn7 sample differs greatly from the others, as a result of its different structure and composition, in agreement with TPD results. Two major peaks at about 360 and 480 °C can be observed, the intensity of the peaks being quite similar. The low temperature peak corresponds to the reduction of MnO_2 to Mn_3O_4, whereas the high temperature peak represents the reduction of Mn_3O_4 to MnO, in agreement with [25].

Using the temperatures of the first component (peak I, see Fig. 2 and Table 2), it is possible to compare the reducibility of all samples. The following trend was obtained: $T_{Mn5} < T_{Mn2} \approx T_{Mn6} < T_{Mn7} < T_{Mn4}$.

As a conclusion, the TPR profiles clearly indicate the major effect of other phases on the reducibility of cryptomelane. The presence of Mn_2O_3 (sample Mn4) decreases the reducibility, while the presence of Mn_3O_4 (sample Mn5) has the opposite effect.

3.1.2. X-ray photoelectron spectroscopy

XPS is a powerful technique for the characterization of surface oxygen species and the determination of surface chemical compositions. In this study, XPS was used for both purposes.

3.1.2.1. O 1s spectra. The manner by which oxygen is bound to metals, in metal oxide catalysts, is most important for their catalytic properties. The O 1s spectrum is frequently used to identify the types of surface oxygen species present in a particular oxide. According to the peak positions, three types of oxygen species can be identified: the low binding energy peak (O_I: 529.8–530.1 eV), which is ascribed to lattice oxygen (O_2^{2-}), the medium binding energy peak (O_{II}: 531.3 eV), assigned to surface adsorbed oxygen (O_2^- or O^-), OH groups and oxygen vacancies; and finally the high binding energy peak (533.0 eV), likely to be associated with adsorbed molecular water [28]. The relative surface oxygen composition plays a key role on the catalytic activity. For example, O_{II} species have higher mobility than lattice oxygen, and some authors correlate the higher activity of a particular catalyst with the higher amount of HO^- groups and oxygen vacancies [9,29]. Fig. 3 shows the O 1s spectra of all samples. The spectra were fitted using the three peaks mentioned above, considering a mixture of Lorentzian and Gaussian curves (all curves have the same shape). The relative abundances of O_I and O_{II} species are listed in Table 3. As expected, the most abundant component in all samples is lattice oxygen (see Table 3), varying between 76% and 72% for Mn5 and Mn6, respectively. On the other hand, the abundance of the O_{II} species ranges between 24% (Mn6) and 20% (Mn4).

3.1.2.2. $Mn2p_{3/2}$ spectra. One of the major problems in the chemistry of non-stoichiometric transition metal oxides is the determination of the oxidation states and the amounts of the different species. This is particularly problematic in the case of manganese oxides, owing to their multiple oxidation states, Mn(II), Mn(III) and Mn(IV), and the overlap of energy ranges for the various oxidation states of manganese. In a previous study [4], the AOS of manganese was determined by XPS, based on a correlation between the binding energies of the doublet separation of Mn3s (ΔE_s) and the AOS, proposed by Galakhov et al. [30]; the corresponding values are presented in Table 1. Here, the relative abundance of Mn(II), Mn(III) and Mn(IV) species for each sample was obtained by studying the $Mn2p_{3/2}$ spectra [31]. The spectra of all samples (not shown) were decomposed into three components corresponding to Mn(II), Mn(III) and Mn(IV) species. Table 3 shows the results obtained. Mn(II) is not detected in samples Mn2, Mn4 and Mn7, in agreement with the X-ray diffraction results. The relative abundances obtained by this method for these samples are roughly in agreement with the average oxidation states (see Table 1).

3.2. Catalytic activity in VOC oxidation

The catalytic performance of all samples was evaluated in the oxidation of ethanol and toluene. In a previous study [4], the same samples were tested in the oxidation of ethyl acetate, and selected results are also included here, for comparison.

3.2.1. VOC oxidation

The ethanol conversion and the conversion into CO_2 as a function of the temperature are presented in Fig. 4. The conversion into acetaldehyde (see Fig. 4b) is also shown, as this compound is the major intermediate in the oxidation of ethanol. For comparative purposes, the temperatures corresponding to 50%, 90% and 100% conversion into CO_2 are summarized in Table 4.

Generally, all the catalysts tested reveal high activity towards the oxidation of ethanol, which is completely converted into CO_2 at temperatures lower than 265 °C. In terms of ethanol conversion, the following performance trend was observed: Mn5 > Mn2 > Mn6 > Mn7 ≈ Mn4. However, the performance of a catalyst should take into account the CO_2 yield and not the global conversion, as the by-products formed could be more toxic than the original reactant. In terms of the temperatures corresponding to 50%, 90% and 100% conversion into CO_2 (see Table 4), the catalysts follow the sequence Mn5 > Mn2 > Mn6 > Mn7 > Mn4. For example, in the presence of the Mn5 catalyst, ethanol achieves full conversion at 215 °C, which is ≈50 °C less than with the Mn4 catalyst. The observed product distribution is clearly indicative of a series reaction scheme, i.e. ethanol is oxidised to acetaldehyde,

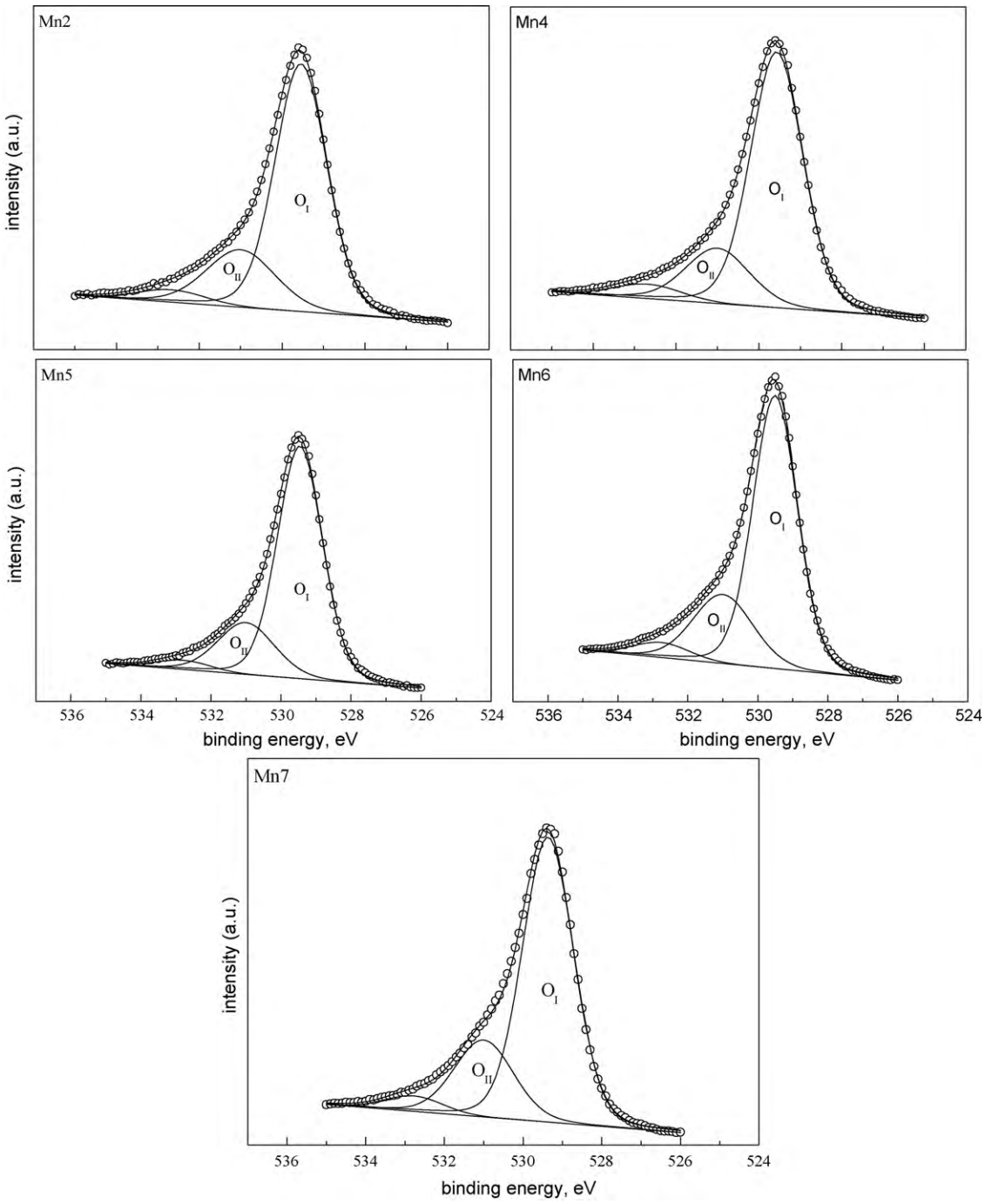

Fig. 3. O 1s XPS spectra of the MnO_x catalysts.

Table 3
XPS results for the MnO_x catalysts.

Sample	O 1s				$Mn2p_{3/2}$					
	O_I[a]		O_{II}[b]		Mn(II)		Mn(III)		Mn(IV)	
	Peak position (eV)	at. (%)	Peak position (eV)	at. (%)	Peak position (eV)	at. (%)	Peak position (eV)	at. (%)	Peak position (eV)	at. (%)
Mn2	529.5	73	531.0	23	–	–	641.4	17	642.3	83
Mn4	529.6	75	531.0	20	–	–	641.9	23	642.2	77
Mn5	529.5	76	531.0	22	640.3	11	641.9	55	643.3	34
Mn6	529.5	72	531.1	24	640.4	12	642.0	57	643.4	31
Mn7	529.4	73	531.0	23	–	–	642.1	18	643.0	82

[a] O_I: lattice oxygen (O_2^{2-}).
[b] O_{II}: surface adsorbed oxygen (O_2^- or O^-), HO^- groups and oxygen vacancies.

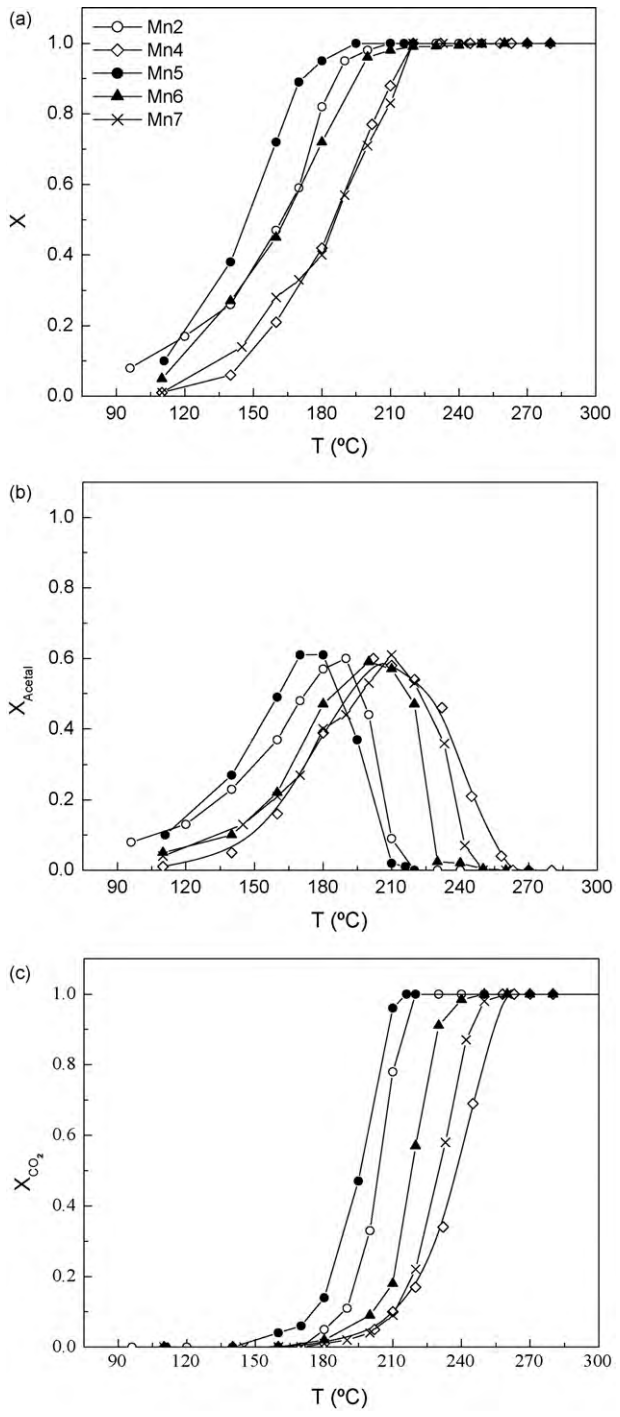

Fig. 4. Light-off curves for ethanol oxidation over the MnO_x catalysts: (a) Ethanol conversion (X); (b) Conversion into acetaldehyde (X_{Acetal}); (c) Conversion into CO_2 (X_{CO_2}). Conversion into acetaldehyde is defined as: $X_{Acetal} = F_{Acetal}/F_{Ethanol,in}$, where F_{Acetal} is the outlet molar flow rate of acetaldehyde at steady state.

and acetaldehyde is further oxidised to CO_2. The contribution of an intermediate step involving the oxidation of acetaldehyde (probably into acetic acid) also seems to occur, especially in the case of Mn6 and Mn4 (this may account for as much as 30% of the total conversion, depending on the temperature).

The corresponding results referring to ethyl acetate [4] are also presented in Table 4. In terms of conversion into CO_2, the following performance trend was observed: Mn5 > Mn2 > Mn6 ≈ Mn7 > Mn4. In this case, the differences between the catalysts are less evident: ethyl acetate is completely oxidised to CO_2 at 213 °C over Mn5, while the complete oxidation occurs at 240 °C in the presence of Mn4. Comparing the VOC conversions, ethanol is slightly more reactive than ethyl acetate [4]. However, the complete oxidation into CO_2 occurs at lower temperatures in the case of ethyl acetate, which may indicate that the by-products formed in the partial oxidation of ethanol (namely acetaldehyde and/or acetic acid) are less reactive than ethyl acetate. Acetaldehyde was also found to be an intermediate product during ethyl acetate oxidation, but its amount is significantly lower than that detected during ethanol oxidation.

In the case of toluene oxidation (see Fig. 5 and Table 4), the catalyst trend is identical to that of ethyl acetate oxidation, although the differences between the catalysts were even less evident in this case. For instance, toluene is completely oxidised into CO_2 at 283 °C over the Mn5 sample, while this oxidation occurs at 300 °C with Mn4. CO_2 is the only product detected from toluene oxidation, at all conversion levels.

Comparing the three VOC studied, toluene is the most resistant to oxidation, requiring temperatures 37–68 °C higher than ethanol for 100% conversion into CO_2. For all VOC studied, Mn5 and Mn2 are the most efficient catalysts, while Mn4 is the worst catalyst of the group. In general, Mn6 and Mn7 have similar performances. Taking into account the characterization results (namely the TPR results), the efficiencies of Mn5, Mn2, Mn7 and Mn4 are in close agreement with the reducibility of the samples (see correlation lines in Fig. 6), revealing the catalytic role of oxygen species from the catalysts. This result is consistent with the oxidation mechanism proposed in the literature for this type of catalysts (MVK mechanism) [3,5,8,10,29]. Sample Mn6 exhibits lower efficiency (see Fig. 6) than what might be expected from the TPR results, so other properties should be taken into account to explain its activity, namely its structure and composition.

XPS results can also shed some light on the mobility of oxygen species. Oxygen vacancies and HO^- groups (O_{II}) play an important role in this context, as they allow the diffusion of lattice oxygen [29]. As can be seen in Table 3, there are no major differences between the relative abundances of O_{II} species in the MnO_x samples, and no correlation can be established. However, Mn4 has the lowest percentage of oxygen vacancies (20%), which can also justify the lowest activity in VOC oxidation.

In order to provide a better understanding of the VOC oxidation mechanism over manganese oxides, some additional experiments were performed, namely TPSR after adsorption of toluene or ethanol, as well as reactions without oxygen in the feed.

Table 4
Catalytic performances expressed as T_{50} (°C), T_{90} (°C) and T_{100} (°C) (temperatures at which 50%, 90% and 100% conversions into CO_2 are obtained).

Sample	Ethanol			Ethyl acetate [4]			Toluene		
	T_{50}	T_{90}	T_{100}	T_{50}	T_{90}	T_{100}	T_{50}	T_{90}	T_{100}
Mn2	204	216	220	200	211	213	252	260	283
Mn4	238	254	263	225	233	240	278	295	300
Mn5	196	208	215	195	206	213	245	258	283
Mn6	219	230	250	217	230	240	272	287	290
Mn7	230	244	258	219	231	240	268	280	300

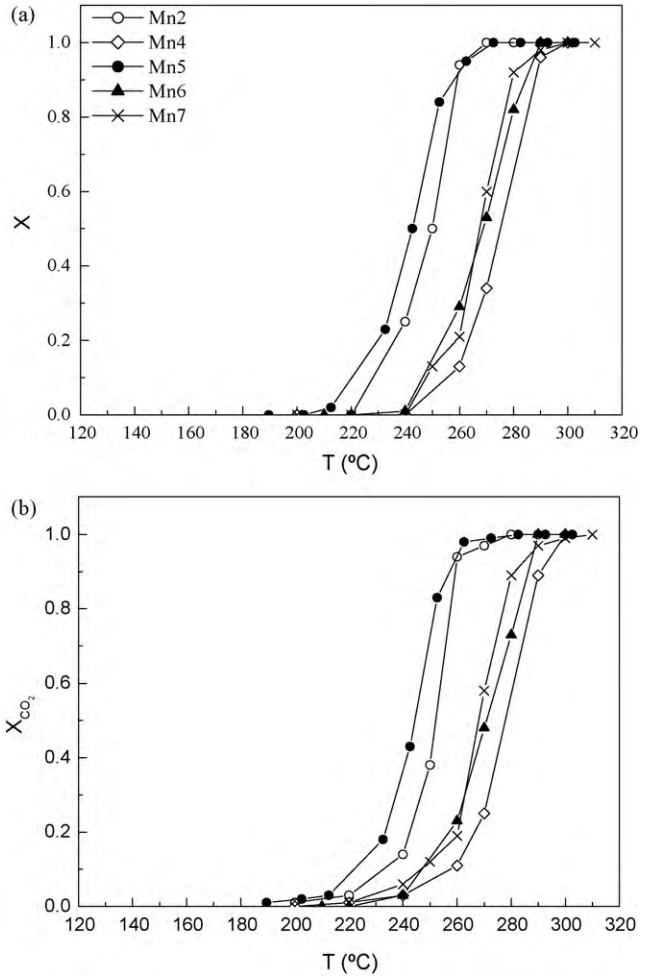

Fig. 5. Light-off curves for toluene oxidation over the MnO_x catalysts: (a) Toluene conversion (X); (b) Conversion into CO_2 (X_{CO_2}).

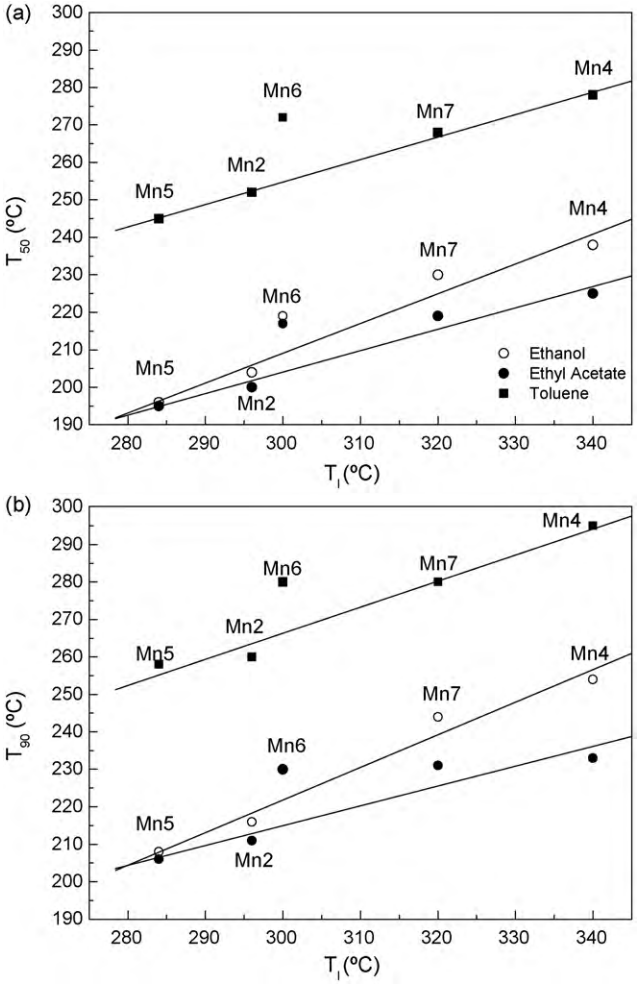

Fig. 6. T_{50} (a) and T_{90} (b) determined for VOC oxidation as a function of the reducibility of the catalysts, expressed as the temperature of the first peak in TPR spectra (T_I (°C)).

3.2.2. Temperature-programmed surface reaction

3.2.2.1. Ethanol. TPSR experiments were performed, in order to analyse the nature of the active sites involved in the oxidation of ethanol over the manganese oxides. The signals of CO_2 (44), water (18), ethanol (31) and acetaldehyde (29) were continuously monitored during the TPSR experiment. CO_2 and water were the only products detected, confirming that lattice oxygen is involved in ethanol oxidation (MVK mechanism). A similar experiment was carried out after adsorption of ethyl acetate in a previous study [5], and the same conclusions were reached.

Fig. 7 shows the CO_2 evolution for all samples. Generally, two significant peaks with a low temperature shoulder (component I) are clearly observed, suggesting the presence of different adsorption-reaction sites. Moreover, in some cases (Mn4 and Mn6), an additional peak at higher temperatures (around 450 °C) was also found, which shows the presence of different adsorbed species.

The adsorption of ethanol over manganese oxides has already been studied by some authors [8,9,11]. Two different adsorption sites were proposed by Peluso et al. [9] in their study of ethanol adsorption over cryptomelane catalysts, in agreement with our own findings. Moreover, infrared studies after adsorption of ethanol at 70 °C [8,11], reveal that the adsorption of ethanol occurs mainly in the form of ethoxides ($H_3C–CH_2–O^-$). As the temperature rises, these ethoxides are converted into acetates, showing different stabilities depending on the structure and composition of the particular manganese oxide. Accordingly, the different component peaks observed in Fig. 7 are the result of the different interactions between ethanol and the catalyst surface, as well as the interactions of some intermediate species involved in the adsorption-reaction pathway of ethanol, namely acetaldehyde and acetic acid. The different surface reactive species involved in the VOC oxidation could be lattice oxygen (O^{2-}) and HO^- groups [7–9,11]. According to the characterization results, the catalyst surface composition (Mn(II), Mn(III), Mn(IV)) plays a key role on the reactivity of lattice oxygen. As a result, the area and intensity of these component peaks differ greatly from sample to sample.

Another important feature related with the TPSR experiment is the amount of CO_2 produced (see Table 5). This value is a measure of the availability to release oxygen and, according to the MVK mechanism, plays a key role on the catalytic activity of manganese oxides.

Table 5
Amounts of CO_2 obtained in the TPSR experiments (a) and in reactions without oxygen in the feed (b).

Sample	CO_2 (μmol/g_{cat})[a]		CO_2 (μmol/g_{cat})[b]	
	Ethanol	Toluene	Ethanol	Toluene
Mn2	550	83	230	158
Mn4	307	48	195	53
Mn5	612	57	238	140
Mn6	464	64	218	100
Mn7	361	103	204	75

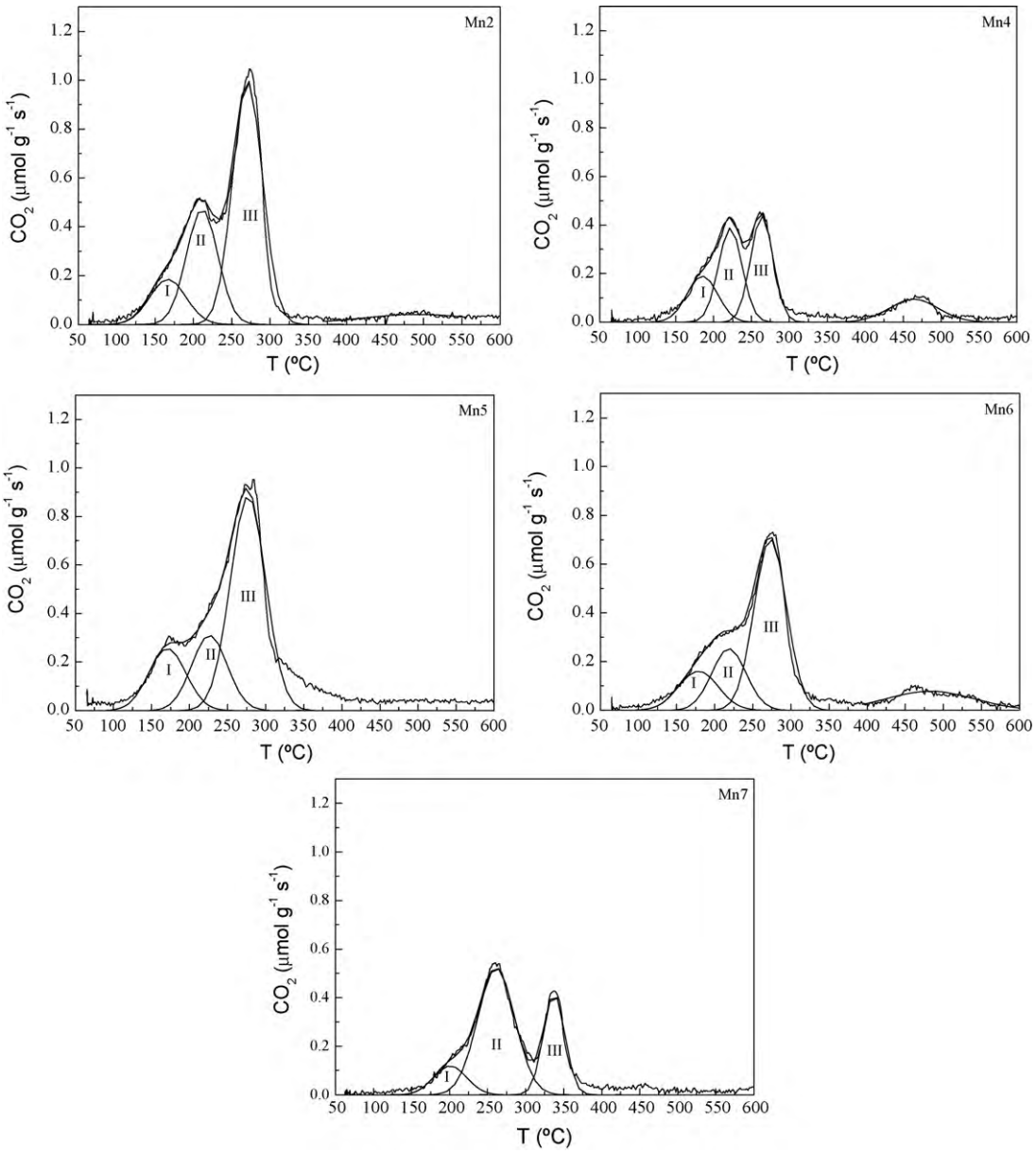

Fig. 7. TPSR experiments (in helium) after adsorption of ethanol at room temperature over the MnO_x catalysts.

Fig. 8 shows that, as expected, there is a clear correlation between the amount of CO_2 produced and the catalytic performance for the total oxidation of ethanol.

3.2.2.2. Toluene. TPSR experiments were also done after adsorption of toluene at room temperature. The signal associated to toluene was also not detected in TPSR, CO_2 and water being the only products detected. However, there are several differences between these results and those obtained with ethanol. The first main difference is related to the shape of the CO_2 evolution curves. One peak (instead of two) was observed in all samples, suggesting that the adsorption/reaction of toluene involves just one type of active site. Furthermore, a much lower amount of CO_2 was measured (see Table 5), and in this case, there is no correlation between that amount and the catalytic performance. This result suggests that adsorbed toluene affects the mobility of the oxygen species, making them less reactive. In a recent report [32], we studied the stability of manganese oxides in the oxidation of toluene, and it was shown that cryptomelane is able to retain toluene at high temperatures (suggesting a strong adsorption).

3.2.3. Reactions without oxygen in the feed

Reactions without oxygen in the feed were also performed for ethanol and toluene, at 210 and 270 °C, respectively. As expected, the oxidation of both VOC takes place in the absence of any gaseous oxygen, which is in agreement with the TPSR experiments. The amounts of CO_2 obtained during ethanol and toluene oxidation are summarized in Table 5, and were correlated with the catalytic performances of all samples (expressed as T_{50} and T_{90}). Fig. 9 shows the results obtained. As can be seen, a significant correlation occurs for both VOC studied, which is consistent with the proposed mechanism.

Following the MVK concept, the re-oxidation of the catalysts is a very important step. Cellier et al. [33] studied the extent of participation of lattice oxygen in the oxidation of n-hexane and trimethylamine over γ-MnO_2. They pointed out that the polariz-

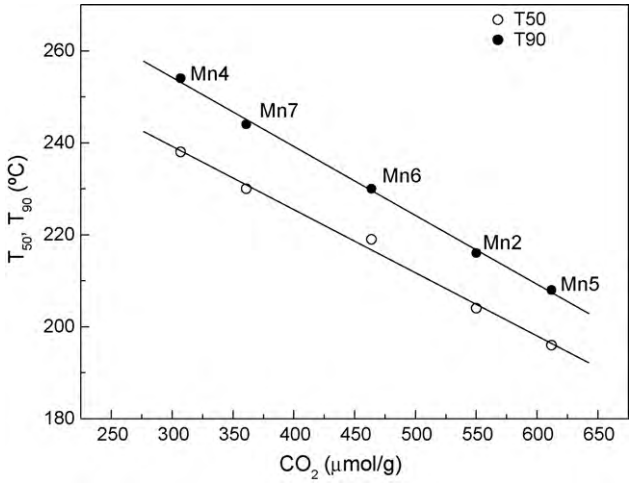

Fig. 8. T_{50} and T_{90} determined for ethanol oxidation as a function of the amount of CO_2 measured during TPSR experiments.

ability of the VOC molecule plays a role in the diffusion of gaseous oxygen and, consequently, in the incorporation of oxygen in the lattice.

In order to study the influence of the type of VOC on the rate of incorporation of oxygen from the gas phase, additional experiments were carried out with the Mn5 sample. In each cycle, prior to the reaction, the catalyst was activated in air at the reaction temperature. The activation time was 10 min in the first cycle, and 5, 2 and 1 min, in the subsequent cycles. The results obtained are summarized in Fig. 10. In the case of ethanol (see Fig. 10a), the molar flow rate of CO_2 produced sharply increases, reaching a maximum value, and then decreasing rapidly. In the last cycle, the total amount of CO_2 produced is significantly lower. During ethanol oxidation, the incorporation of oxygen from the gas phase is very fast, and only 2 min of treatment are enough to re-oxidise the active sites. In the case of toluene (see Fig. 10b), the re-oxidation of the catalyst is more difficult, and 5 min are not enough to activate the catalyst. The shapes of the curves differ greatly from those obtained in the case of ethanol, the molar flow rate of CO_2 measured decreasing at a very slow rate for an extended period of time. The slow incorporation of oxygen on the active sites is assumed to explain the lower conversions.

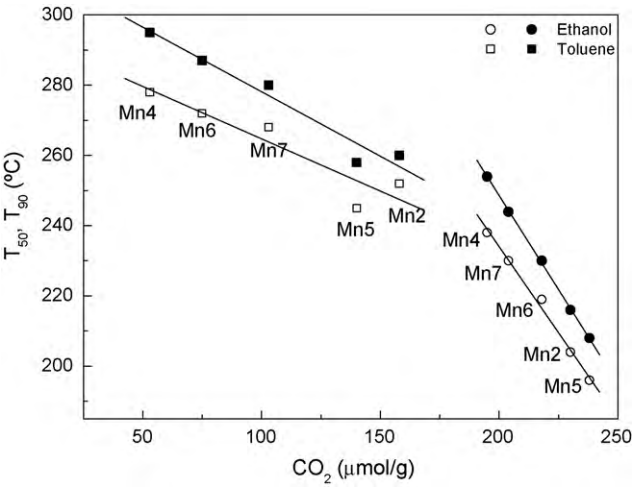

Fig. 9. T_{50} (open symbols) and T_{90} (filled symbols) determined for ethanol and toluene oxidation as a function of the amount of CO_2 obtained in the reactions without oxygen in the feed.

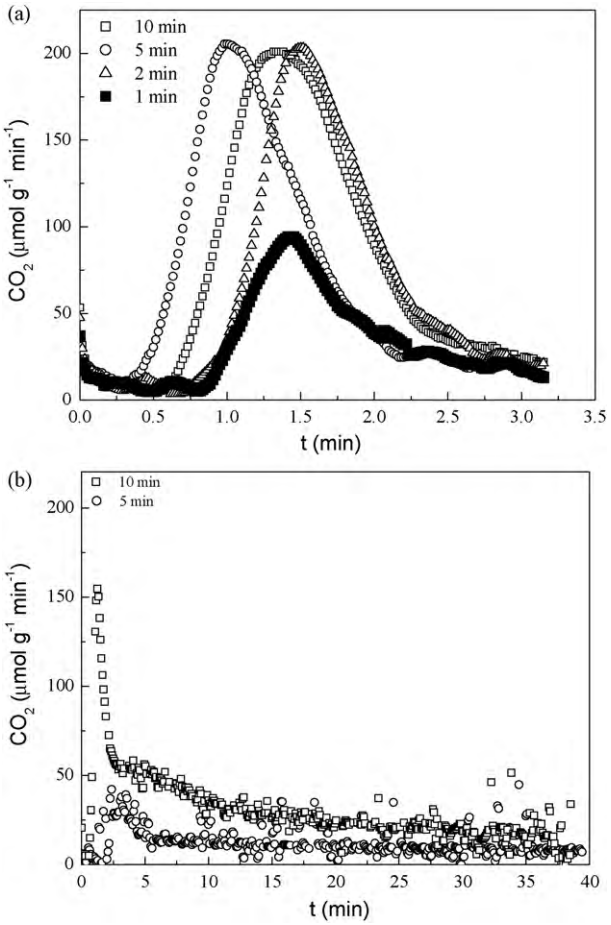

Fig. 10. Influence of the activation time on the conversion into CO_2 over Mn5 without oxygen in the feed: (a) Ethanol at 220 °C; (b) Toluene at 270 °C.

4. Conclusions

The main conclusions that can be drawn from this study are:

- Characterization results by XPS, TPD and TPR show that the oxygen species present in MnO_x samples have different mobility and reactivity, as a result of their different structure and composition.
- All samples were very active for the total oxidation of ethanol, ethyl acetate and toluene. The following reactivity trend was observed: Ethyl Acetate > Ethanol > Toluene.
- Cryptomelane was found to be very active in VOC oxidation. Its performance is significantly affected by the presence of other phases, namely, Mn_2O_3 and Mn_3O_4. Mn_3O_4 improves the catalytic activity due to the increase of the reactivity and mobility of lattice oxygen, while Mn_2O_3 has the opposite effect. These results show that the reducibility and reactivity of lattice oxygen play a key role on the activity of manganese oxides.
- Temperature-programmed surface reaction studies after adsorption of ethanol or toluene over MnO_x samples show that the interaction of these molecules with the catalyst surface is quite different. In the case of ethanol, two types of adsorption/reaction sites are involved, while in the case of toluene just one type of active site is evident. Moreover, in the case of ethanol, the amounts of CO_2 obtained during these experiments are correlated with the catalytic performances.
- Reactions without oxygen in the feed, after different activation conditions, suggest that the incorporation rate of oxygen is slower in the case of toluene. This may explain its lower reactivity. Strong correlations between catalytic performance (measured by T_{50} or

T_{90}) and CO_2 produced in these experiments were observed, both for ethanol and toluene, in agreement with a Mars and van Krevelen mechanism.

Acknowledgements

This work was supported by Fundação para a Ciência e a Tecnologia (FCT) and FEDER under Program COMPETE (Project PTDC/AMB/69065/2006). V.P.S. acknowledges the grant received from FCT (SFRH/BD/23731/2005). The authors also acknowledge Dr. Carlos M. Sá (CEMUP) for assistance with XPS analyses.

References

[1] J. Luo, Q. Zhang, A. Huang, S.L. Suib, Micropor. Mesopor. Mater. 35–36 (2000) 209.
[2] J. Cai, J. Liu, W.S. Willis, S.L. Suib, Chem. Mater. 13 (2001) 2413.
[3] J. Luo, Q. Zhang, J. Garcia-Martinez, S.L. Suib, J. Am. Chem. Soc. 130 (2008) 3198.
[4] V.P. Santos, M.F.R. Pereira, J.J.M. Órfão, J.L. Figueiredo, Top. Catal. 52 (2009) 470.
[5] V.P. Santos, M.F.R. Pereira, J.J.M. Órfão, J.L. Figueiredo, Appl. Catal. B-Environ. 88 (2009) 550.
[6] M.I. Dominguez, P. Navarro, F. Romero-Sarria, D. Frias, S.A. Cruz, J.J. Delgado, M.A. Centeno, M. Montes, J.A. Odriozola, J. Nanosci. Nanotechnol. 9 (2009) 3837.
[7] L. Lamaita, M.A. Peluso, J.E. Sambeth, H. Thomas, G. Mineli, P. Porta, Catal. Today 107–08 (2005) 133.
[8] L. Lamaita, M.A. Peluso, J.E. Sambeth, H.J. Thomas, Appl. Catal. B-Environ. 61 (2005) 114.
[9] M.A. Peluso, L.A. Gambaro, E. Pronsato, D. Gazzoli, H.J. Thomas, J.E. Sambeth, Catal. Today 133–135 (2008) 487.
[10] S.L. Suib, J. Mater. Chem. 18 (2008) 1623.
[11] M.A. Peluso, E. Pronsato, J.E. Sambeth, H.J. Thomas, G. Busca, Appl. Catal. B-Environ. 78 (2008) 70.
[12] Y.F. Shen, R.P. Zerger, R.N. Deguzman, S.L. Suib, L. McCurdy, D.I. Potter, C.L. Oyoung, Science 260 (1993) 511.
[13] S. Ching, S.L. Suib, Comments Inorg. Chem. 19 (1997) 263.
[14] S.L. Brock, N.G. Duan, Z.R. Tian, O. Giraldo, H. Zhou, S.L. Suib, Chem. Mater. 10 (1998) 2619.
[15] Q. Feng, K. Yanagisawa, N. Yamasaki, J. Porous Mater. 5 (1998) 153.
[16] R.N. Deguzman, Y.F. Shen, E.J. Neth, S.L. Suib, C.L. Oyoung, S. Levine, J.M. Newsam, Chem. Mater. 6 (1994) 815.
[17] K.A. Malinger, Y.S. Ding, S. Sithambaram, L. Espinal, S. Gomez, S.L. Suib, J. Catal. 239 (2006) 290.
[18] S. Ching, J.L. Roark, N. Duan, S.L. Suib, Chem. Mater. 9 (1997) 750.
[19] Y.S. Ding, X.F. Shen, S. Sithambaram, S. Gomez, R. Kumar, V.M.B. Crisostomo, S.L. Suib, M. Aindow, Chem. Mater. 17 (2005) 5382.
[20] Y.G. Yin, W.Q. Xu, R. Deguzman, S.L. Suib, C.L. Oyoung, Inorg. Chem. 33 (1994) 4384.
[21] Y.G. Yin, W.Q. Xu, Y.F. Shen, S.L. Suib, C.L. Oyoung, Chem. Mater. 6 (1994) 1803.
[22] Y.G. Yin, W.Q. Xu, S.L. Suib, C.L. Oyoung, Inorg. Chem. 34 (1995) 4187.
[23] B. Levasseur, S. Kaliaguine, Appl. Catal. B-Environ. 88 (2009) 305.
[24] D.L. Bish, J.E. Post, Am. Miner. 74 (1989) 177.
[25] F. Kapteijn, L. Singoredjo, A. Andreini, J.A. Moulijn, Appl. Catal. B-Environ. 3 (1994) 173.
[26] W. Gac, Appl. Catal. B-Environ. 75 (2007) 107.
[27] R. Xu, X. Wang, D.S. Wang, K.B. Zhou, Y.D. Li, J. Catal. 237 (2006) 426.
[28] K. Jiratova, J. Mikulova, J. Klempa, T. Grygar, Z. Bastl, F. Kovanda, Appl. Catal. A-Gen. 361 (2009) 106.
[29] H. Chen, A. Sayari, A. Adnot, F. Larachi, Appl. Catal. B-Environ. 32 (2001) 195.
[30] V.R. Galakhov, M. Demeter, S. Bartkowski, M. Neumann, N.A. Ovechkina, E.Z. Kurmaev, N.I. Logachevskaya, Y.M. Mukovskii, J. Mitchell, D.L. Ederer, Phys. Rev. B 65 (2002) 4.
[31] Y.J. Wei, L.Y. Yan, C.Z. Wang, X.G. Xu, F. Wu, G. Chen, J. Phys. Chem. B 108 (2004) 18547.
[32] V.P. Santos, S.S.T. Bastos, M.F.R. Pereira, J.J.M. Órfão, J.L. Figueiredo, Catal. Today (2010), doi:10.1016/j.cattod.2009.12.005.
[33] C. Cellier, V. Ruaux, C. Lahousse, P. Grange, E.M. Gaigneaux, Catal. Today 117 (2006) 350.